FirePhysChem 4 (2024) 283–294

Contents lists available at ScienceDirect

FirePhysChem

journal homepage: http://www.keaipublishing.com/cn/journals/firephyschem/

# Novel approach for preparation of the energy-safety balanced cocrystals of attractive nitramines *via* coagglomeration

Veerabhadragouda B Patil*, Svatopluk Zeman

*Institute of Energetic Materials, Faculty of Chemical Technology, University of Pardubice, Pardubice CZ532 10, Czech Republic*

ARTICLE INFO

*Keywords:*
Co-agglomeration
Co-crystals
Detonation parameters
Impact sensitivity
Nitramines

ABSTRACT

Co-agglomeration unique crystal engineering approach; in which the co-precipitated micro-particles of nitramines with other energetic materials co-agglomerated by the slurry method; to modify the energetic properties of attractive nitramines like CL20, HMX, BCHMX, and RDX etc. The interesting properties and structural modifications in newly prepared co-agglomerated crystals (CACs) interesting one are discussed here. There are notable variations in the crystal morphologies and packing of crystals, including key properties like relatively high density, melting point, impact sensitivity, and detonation properties. These CACs are in the overwhelming and majority showing properties like co-crystals. Apart from these aspects, co-agglomeration provides a huge opportunity to tune the key properties and performance of existing energetic materials and is easy to scale-up for the industrial level. These preliminary results also suggest that chemical engineering factors are involved in the preparation of CACs and have tremendous improvements than the conventional crystallization. With technological optimization this method can be employable industrial scale production.

## 1. Introduction

High energy materials (HEMs) - explosives are one of the most essential because they release large amounts of energy and gases rapidly [1]. Despite their production and handling risks, these materials proved indispensable in military and civilian uses. Evolution has been slow for over 1200 years; black powder prevailed until the early 20th century. In this scenario, from 2,4,6-trinitrotoluene (TNT) to 1,3,5,7-tetranitro-1,3,5,7-tetrazocane (HMX) and 2,4,6,8,10,12-hexanitro-2,4,6,8,10,12-hexaazawurtzitane (CL-20), the first, second, and third generation HEMs, respectively, the detonation velocity (D) improved by 30% by the end of the century. New HEMs are being synthesized, but their performance and sensitivity cannot exceed those of older HEMs [2–5]. Because of CHNO limitations in organic HEM systems [6], newly synthesized HEMs are inefficient and unusable [7], contradicting coherent property Energy & Safety [7,8]. Research emphasizes safer explosives to prevent this conflict in upcoming HEMs. As it thus seems, possibilities of a chemical way to a HEMs by the synthesizing of a new family of energetic materials are relatively saturated.

As a result, an alternate strategy for altering the characteristics of established explosives was opted for. Crystal engineering of HEMs, which focuses on the altering of their properties through co-crystallization [9–11], developed out of this context. There is a tremendous development in cocrystallization of energetic materials methodologies, for example cocrystallization of energetic materials with non-energetic materials, as well as with energetic materials.

The resulting crystals may have a higher density ($\rho$) and packing coefficient than the original components (coformers), but their melting temperature ($T_m$) and thermal breakdown onset ($T_d$) are often lower. The resulting energetic cocrystals (ECCs), with the right preparation technology, can be more resistant to mechanical stimuli and have better performance than their coformers, as has been established in previous studies [9–11]. The literature is predominated by procedures requiring comparatively larger volumes of solvents [12], such as evaporation of solutions, application of the solvent/antisolvent system, and crystallization under cooling. The authors also evaluated ultrasonic-assisted solvent/antisolvent crystallizations, spray drying, and electro-spraying as potential best practices [10]. In addition, most of the techniques discussed here also have downsides, such as increased solvent usage, prolonged cocrystal preparation durations, quantitative limits, or inapplicability to specific coformers. However, despite their evident benefits, these methods are typically only suitable for producing small quantities /laboratory scale of co-crystals. Grinding methods, melting/condensation crystallization, resonant acoustic method, self-assembly method, slurry method, and method with solvent-suspension are all examples of ways to prepare

* Corresponding author.
*E-mail address:* iamveerabhadraa@gmail.com (V.B. Patil).

https://doi.org/10.1016/j.fpc.2024.03.003
Received 22 January 2024; Received in revised form 5 March 2024; Accepted 5 March 2024
Available online 6 March 2024

ECCs that do not require solvents or only require small quantities of them [12].

The fact that nano- and micro-particles of HEMs [9,12,13] agglomerate easily (mostly RDX and HMX) has been verified by Zhao et al. [14]. during the preparation of ECCs from the 1,3,5-trinitro-2,4,6-triaminobenzene (TATB) and HMX nanoparticles by in their co-agglomeration in a hot water under pressure. In our technique, the co-agglomeration takes place in a low-solubility solvent (either aprotic or protogenic) such that the coformers can be co-crystallized in suspension ("slurry method" of cocrystallization).

In the present case, the initial mixture of the coformers was prepared by precipitation from their common solution by anti-solvent. Using co-agglomeration with polynitroarenes [15–21], with sterically hindered nitramines molecules [17], i.e. CL20 and BCHMX, and with electrically conducting polyaniline (PANi) [20,22], this technique is very helpful in creating co-agglomerated crystals (CACs) - characteristic cocrystals of the attractive nitramines, as well as adoptable in application large scale [21]. In this short review of the coagglomeration method results, the presented details about successful efforts to prepare CACs and their properties from the perspective of their detonation properties (energy) and sensitivities (safety) in order to demonstrate their utility.

## 2. Experimental part

### 2.1. Materials & methods

The preparation of co-agglomerated crystals (CACs) with specific energetic coformers (shown Fig. 2(a)–(d)) and the aforementioned attractive nitramines (shown Fig. 2(c)–(h)) was conducted using a primarily two-step procedure [15].

(1) First step - the co-precipitates are prepared by employing the rapid solvent-antisolvent method. This method involves introducing a solution containing co-formers, which do not necessarily possess a defined crystallography and can be obtained directly from their production after stabilization (e.g., introducing water into the acetonic solution).
(2) Second step - Co-agglomeration strategy involves combining a small quantity of solvent with a co-precipitate, resulting in a well-mixed slurry (in which components exhibit low solubility in the solvent). Subsequently, the slurry is subjected to heating for a specific duration, reaching a temperature around the boiling point of the solvent.

The acquired CACs were dried, subsequently labeled, and subjected to a comprehensive analysis for morphology and phase purity, and also underlying intermolecular changes in both coformers after undergoing coagglomeration were described. The coagglomeration method works as controlled cocrystallization as compared to earlier literature reported methods and obtained detonation parameters (Table 3).

## 3. Results and discussions

### 3.1. The factors shaping the coformers cohesiveness in crystal lattice of CACs

Usually, the individual coformers exhibits hydrogen bonding between them to form a stabilized crystal lattice. In cocrystals the coformers are connected by attractive intermolecular / interlayered electrostatic interactions (shown Fig. 1) [20–22].

These interactions help to stabilize both coformers (Fig. 2) in the single crystal lattice i.e., in cocrystal form. According to the component and structural types of the objects involved in the interactions, intermolecular interaction (noncovalent interaction) is divided into van der Waals interaction (dispersion interaction) and electrostatic interaction (Coulomb interaction). Chemically, they are also be referred to as hydrogen bonding (HB), halogen bonding, or stacking [20,23,24,26,27].

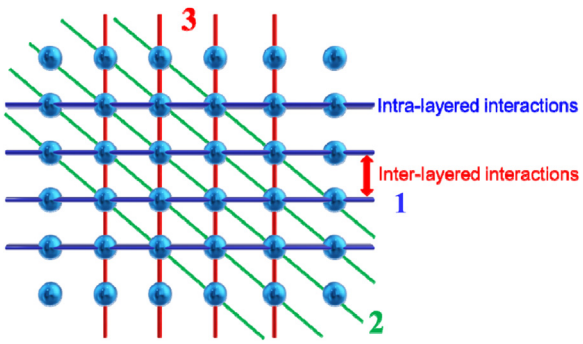


**Fig. 1.** Schematic of the intra- and inter-layered intermolecular interactions. The thickness of the lines represents the strength of intermolecular interactions: the thicker line suggests stronger interactions (Recreated from Ref. [23]).

Spectral and powder X-ray diffraction measurements have demonstrated the creation of short contacts of the N-O—H type, including stacking of benzene rings with selected coformers, hydrogen bonding, and van der Waals forces of attraction (which primarily occur between $NO_2$, N-N (nitramines), and C-H). The stability of the crystal lattice is increased by these intra- and intermolecular interactions (for the PANi coformer see a charge transfer complex type of interaction in Fig. 2(i)).

As a result of these intra and intermolecular interactions between coformers and nitramines (structures shown in Fig. 2 for pure coformers) exhibited observable above mentioned changes, which suggests that molecules of coformers at particular molar ratio enter into the nitramines crystal lattice. These changes are described in detail in recent publications [15–22] and results summarized briefly as follows.

### 3.2. CACs of attractive nitramines with DATB and TATB

Both 1,3-diamino-2,4,6-trinitrobenzene (DATB) and 1,3,5-triamino-1,3,5-trinitro benzene (TATB) lead to the formation of co-agglomerates (CACs) with the nitramines (shown Fig. 2(e) and (f)), in which HMX presents in its $\delta$-form and CL-20 in its $\beta$-form [14,15]; the $\delta$-HMX stabilization in these CACs is particularly interesting, since the lifetime of this pure isomer is only 12 h [30]. Whereas using DATB yielded CACs with a density of at most 99% of the theoretical density of the mixed crystal, the TATB CACs densities are higher than those using the pure nitramines (including $\beta$-CL-20). The sensitivity is quite strongly reduced in the TATB CACs (15–50 J) compared to their DATB analogues (4–12 J). Detonation parameters of CACs containing DATB and TATB are logically lower than those of the starting nitramines. The detonation energies of these mixed crystals are higher than would be expected from the respective percentage of the co-formers. The most interesting of the CACs studied appears to be HMX/TATB ($D$ = 9332 m/s) which in the formulation used here, has a slightly increased density ($\rho$ = 1.909 g/cm$^3$) with only slightly reduced detonation parameters compared to pure HMX ($\rho$ = 1.902 g/cm$^3$, $D$ = 9404 m/s), while its impact resistance is extremely high (50 J). This CACs, together with RDX/TATB co-agglomerate, could be suitable filler for ammunition objects with high vulnerability resistance.

### 3.3. CACs of CL20 and BCHMX

The CACs of sterically crowded molecules CL20/BCHMX (shown Fig. 2(c) and (d)) took long time efforts finally stabilized form obtained [17], here most important things are used medium of co-agglomeration and the molar ratio of coformers. This can yield a co-crystal with clearly lower impact sensitivity (14.9 J for the $\beta$-CL-20/BCHMX molar ratio = 1.8) than that of pure $\varepsilon$-CL-20 (13.2 J) and of pure BCHMX (3 J) (shown in Tables 2 and 3). The density of the studied co-agglomerates (CACs) achieves 99.5% of the theoretically calculated ones and the density of the coformers at the molar ratios used reaches 99.6% of the

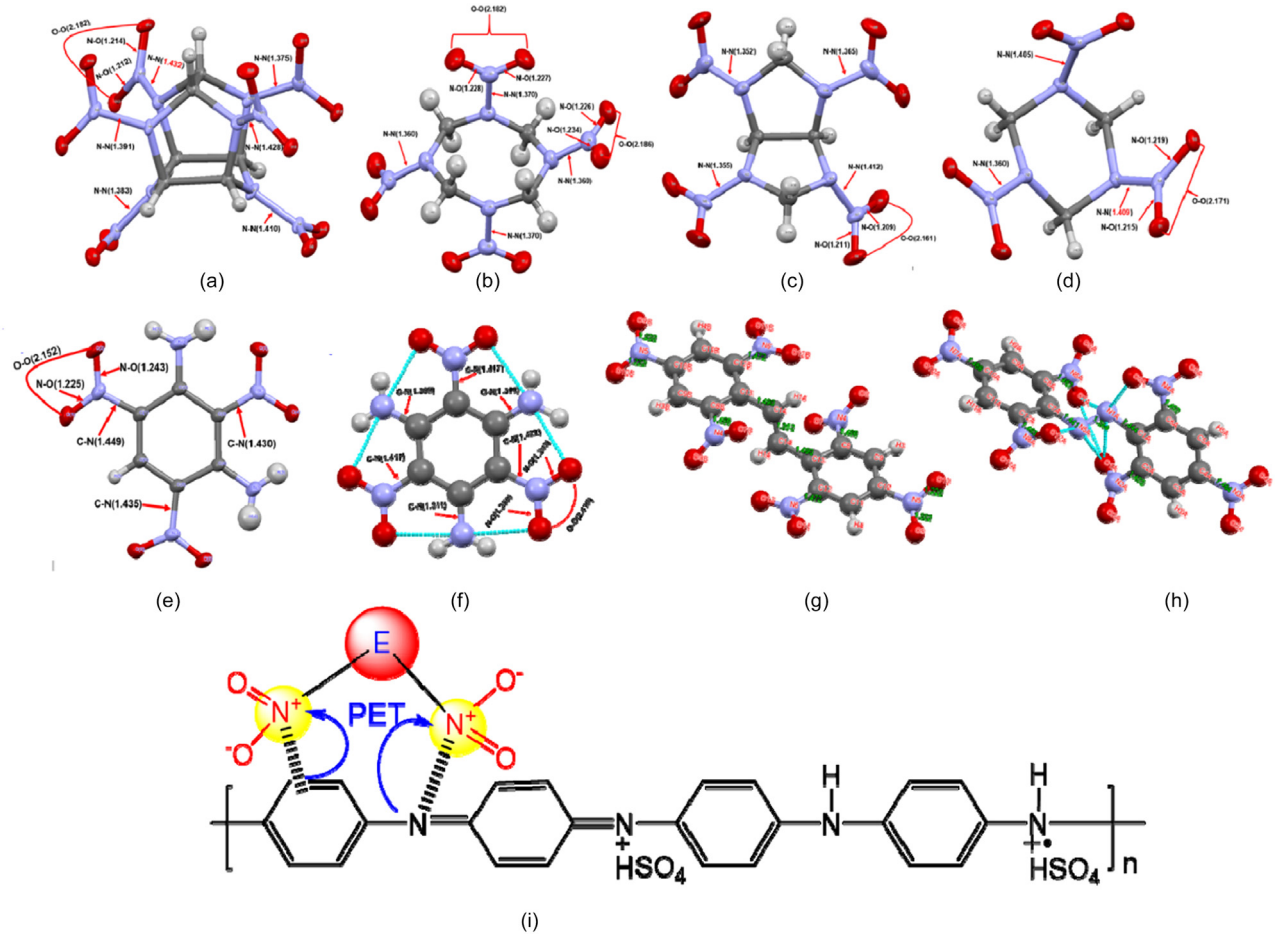


**Fig. 2.** 3D molecular structures of attractive nitramines (a)-(d) and coformers used in CACs preparations. (a) CL20. (b) HMX. (c) BCHMX. (d) RDX and coformers used for CACs. (e) DATB. (f) TATB. (g) HNS. (h) HNAB [15–21]. (i) 2D Emeraldine salt of PANi "E" – attractive cyclic nitramine i.e., it denotes formation of charge transfer complex with (a), (b), (c), and (d) [28,29].

$\beta$-CL-20 crystal density. The CACs has shown that CL-20 is present in them as its ß-modification; in one sample, obtained by classical co-crystallization, have both $\alpha$- and $\beta$-modifications.

The CACs studied have lower detonation energies than would be consistent with the percentage of individual coformers in these crystals; this is a new finding, which does not correspond to the general view about the detonation parameters of explosive mixtures. The application of the most sensitive CACs (1.2 J) as a detonator primer did not exhibit the required acceleration capabilities in the given detonator design. However, a comparison with literature data (Table 3) shows that the CACs and CCs of this type could have advantageous applications in propellants because $\beta$-CL-20 is morphologically stable in these co-mixed crystals.

### 3.4. CACs of attractive nitramines with HNS and HNAB

The CACs with the 2,2′,4,4′,6,6′-hexanitro-2,2′,4,4′,6,6′-stilbene (HNS) coformer are finer grained than those with the 2,2′,4,4′,6,6′-hexanitro- 2,2′,4,4′,6,6′- azobenzene (HNAB) one (shown Fig. 2(g) and (h)). CACs containing HNAB seem to be more perfect than CACs containing HNS [19]. However, impact sensitivity of the second mentioned ones is generally lower; the dominant sample is HMX/HNS with the molar ratio of 1.00/0.11 and the impact sensitivity of 47 J. The study of the surface morphology of these crystals has shown their microporous structure, which is not significantly reflected into their crystal density. These CACs probably contain porous micro/nano crystalline clusters of HNS (for the pure HNS recently similar structure described in Ref. [31]). Three other CACs (RDX/HNS, RDX/HNAB and BCHMX/HNAB) had higher impact resistance than that exhibited by their original pure coformers. For CL20, however, the entry of HNS or HNAB into its crystal lattice is destabilizing.

In these CACs the HMX is present in its $\delta$-form, CL-20 in its $\beta$-form and the trans-HNS molecule changes its conformation to cis-form. On the basis of FTIR and Raman spectral studies shown there are more intense intermolecular interaction between HNS and nitramines (especially through the hydrogen bonds formed by the hydrogen atoms of the –CH=CH– bridge) and in the case of $\delta$-HMX also thanks to its spatial compatibility with cis-HNS molecules. The most interesting CAC from those studied appears to be the already-mentioned HMX/HNS with the molar ratio of 1.00/0.11 and the microporous structure of its crystals, whose calculated detonation velocity is of 8.98 km/s for $\rho$ = 1.8778 g/cm$^3$ (compare with 9.40 km/s for $\beta$-HMX). The combination of HMX and HNS molecules thus appears to be advantageous. The CACs studied, with the exception of the ones containing CL-20, may be applied as secondary fillers of special detonators and, after the verification of their pressability, also as fillers of various ammunition objects.

### 3.5. CACs of attractive nitramines with PANi

After successfully preparing the CACs of the Energetic-Energetic molecules category, coagglomeration extended to check feasibility

**Table 1**
Particle size measurements [15–22].

| Sr No's | Code design | Solvent system of coprecipitation | Surface area ($m^2$/kg) | *Dv*(50) (μM) | *Dv*(90) (μM) | Refs. |
|---|---|---|---|---|---|---|
| 1 | 32 HMX/TATB | DMFA/water | 3160 | 2.45 | 12 | [15] |
| 2 | 33 BCHMX/TATB | DMFA/water | 3765 | 1.69 | 12.8 | [15] |
| 3 | 34 CL-20/TATB | DMFA/water | 5633 | 1.77 | 3.88 | [15] |
| 4 | 35 RDX/TATB | DMFA/water | 4614 | 12.5 | 43.1 | [15] |
| 5 | BCHMX/DATB-Cp1 | NMP/water | 621.1 | 14.1 | 33.3 | [15] |
| 6 | BCHMX/DATB-Cp2 | NMP/water + Surfactant | 70.6 | 127 | 1809 | [15] |
| 7 | RDX/DATB-Cp3 | NMP/water | 433.5 | 23.4 | 53.3 | [15] |
| 8 | δ-HMX/DATB-Cp4 | DMSO/water | 665.7 | 12.1 | 23.6 | [14] |
| 9 | ß-CL-20/DATB-Cp5 | DMSO/water | 1779 | 22.6 | 58.1 | [14] |
| 10 | CCs2 CL20/BCHMX | Ethyl-formate/hexane | 1106 | 16.9 | 64.8 | [16] |
| 11 | S4 CL20/BCHMX | DMSO/water | 1468 | 15.4 | 65.2 | [16] |
| 12 | S5 CL20/BCHMX | DMSO/water | 1007 | 16.7 | 50.4 | [16] |
| 13 | S4LV CL20/BCHMX | DMSO/water | 861 | 16.3 | 58.8 | [16] |
| 14 | S4LZ CL20/BCHMX | DMSO/water | 3171 | 3.22 | 9.48 | [16] |
| 15 | S5LV CL20/BCHMX | DMSO/water | 927 | 15.6 | 37.5 | [16] |
| 16 | 3 HMX/HNS | DMSO/water | 1596 | 5.92 | 20.1 | [18] |
| 17 | 6 HMX/HNS | DMSO/water | 1973 | 6.49 | 26.7 | [18] |
| 18 | 8 HMX/HNS | DMSO/water | 1732 | 4.52 | 13.1 | [18] |
| 19 | 17 RDX/HNS | DMF/water | 2089 | 6.05 | 23.6 | [18] |
| 20 | 18 CL-20/HNS | DMF/water | 1772 | 8.76 | 34.2 | [18] |
| 21 | 19 BCHMX/HNS | DMF/water | 1547 | 6.87 | 20.2 | [18] |
| 22 | 20 RDX/HNAB | DMK/hexane | 441.3 | 27.2 | 54.8 | [18] |
| 23 | 21 BCHMX/HNAB | DMK/hexane | 629.4 | 19.8 | 61.8 | [18] |
| 24 | 22 CL-20/HNAB | DMK/hexane | 1056 | 10.8 | 25.1 | [18] |
| 25 | 31 HMX/HNAB | DMK/hexane | 912.4 | 15.8 | 41.9 | [18] |
| 26 | 38 HMX/HNAB | DMK/hexane | 792 | 15.8 | 62.9 | [18] |
| 27 | 39 CL-20/HNAB | DMK/hexane | 872.9 | 12.3 | 33 | [18] |
| 28 | 57 CL20/ PANi | DMSO/water | 1764 | 6.79 | 40.5 | [20] |
| 29 | 58 HMX/PANi | DMSO/water | 788.6 | 18.7 | 80.6 | [20] |
| 30 | 59 BCHMX/PANi | DMSO/water | 1233 | 8.35 | 40.1 | [20] |
| 31 | 60 RDX/PANi | DMSO/water | 1126 | 9.66 | 40.4 | [20] |

of the method nonen ergetic polymeric moiety with these attractive nitramines [20]. Obtained results are interesting with polyaniline (PANi), which shown effective influence in these attractive nitramines (shown Fig. 2(i)). As usual the polymorphic changes observed exhibited α-HMX and β-CL20 after interacting with polymer chain. These attractive nitramines formed a charge transfer complex with PANi chain [23,26], its interesting changes further confirmed by fluorescence quenching and quantum yield. In crystalline form the PANi moiety coated on surface of the nitramines crystals which further leads to thermal, mechanical/impact stability in corresponding CACs, however due to conductive nature PANi electric they are spark sensitive. In all these nitramine complexes showed an increased sensitivity to electrical spark, (57) CL20/PANi 40.9 mJ; (58) α-HMX/PANi 37.9; (59) BCHMX/PANi 23.2 mJ and (60) RDX/PANi 21.4 mJ. Also found laser (29 mV with 10×/0.25 grating) sensitive in Raman measurements. From the point of view of performance in the studied nitramines is more interesting RDX/PANi complex ($D$ = 8744 m/s) with a slightly increased density ($\rho$ = 1.8295 g/$cm^3$), slightly reduced calculated detonation parameters compared to pure RDX ($\rho$ = 1.810 g/$cm^3$, $D$ = 9014 m/s), with also a good impact resistance of 21 J. The most resistant against impact is α-HMX/PANi (31.01 J), followed by remaining CACs (Tables 2 and 3). These PANi coagglomerates could be suitable primary components for electrical initiators.

### 3.6. Particle size and morphology of CACs

Particles size analysis of CACs (Table 1) shown the effect of co-agglomeration for attractive nitramines with enhancements in their surface areas. For understand influence both co-precipitation and co-agglomeration some samples particle analysis for co-precipitates (in Table 1 samples codes end with P) also carried followed by final product CACs. Regarding the size of the CACs determined size and specific surface area, especially for nitramines with sterically crowded molecules, i.e., BCHMX and CL20, there is only a slight increase of its value during the agglomeration process; the spatial compatibility of the angular molecule BCHMX and the globular one β-CL20 have to be logically quite limited [17].

The CACs of RDX and HMX co-agglomerate well, which is within expectations. The polynitroaromatic coformers, co-agglomeration is most strongly suppressed by TATB, which is also logical (due to relatively strong non-covalent bonds of the N-O—H-N type [15–21]).

In terms of SEM-based crystal quality assessment, the best CACs were β-CL20/BCHMX with a molar ratio of 1.8 components (also in terms of impact sensitivity) [17], followed by nitramine co-agglomerates with HNAB [19]. On the other hand, in the case of a δ-HMX/HNS co-agglomerate with a molar ratio of 1.00/0.42, which is demonstrably microporous (see Fig. 3 sample code 8) without significant reflect into their crystal density [19]; these microporous structure are caused by HNS crystal morphology [31].

### 3.7. Impact sensitivity

The well-known observation of Dr. Licht [32] that high performance explosives usually have high sensitivity was developed over time into a semilogarithmic relationship [33] between impact sensitivity and the energy content of explosives, represented by the enthalpy of formation which is presented by Figs. 4 and 5.

It can be seen that the stabilizing effect of incorporating TATB into the HMX crystal lattice (Serial No. 2 in Table 1) can practically match with the same effect of HNS (Serial No. 25 in Table 1). In doing so, both types of CACs, in terms of the FESEM image (Fig. 3), give the impression of imperfect crystals. This interesting effect is still waiting for explanation. It may be due to flexible crystal formation which are resisting impact becoming pallet. The flow of dependencies in Fig. 5 is consistent with Licht's rule, except that there is a known, as yet unexplained exception for pure RDX, HMX and CL20 [34].

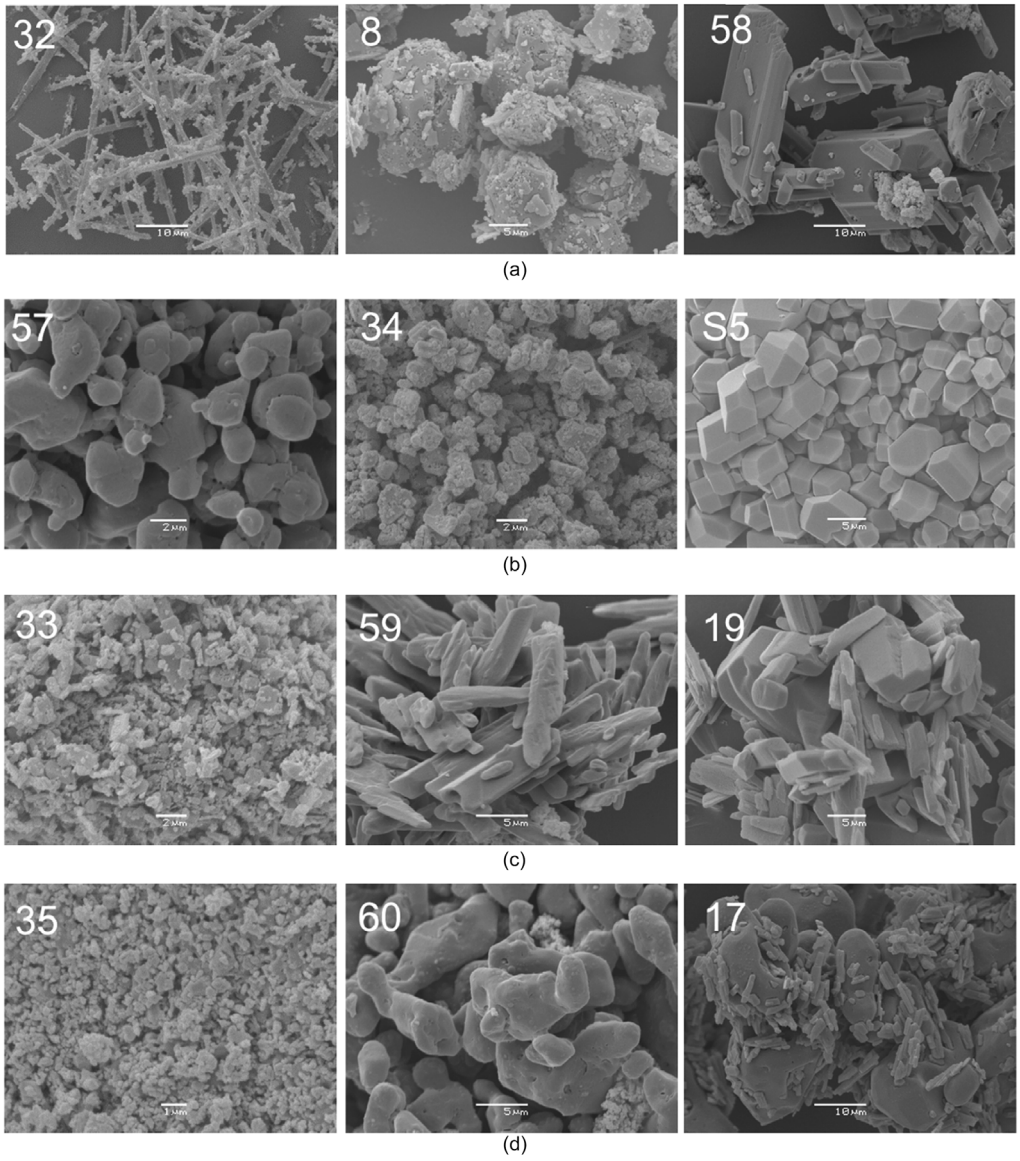


**Fig. 3.** FESEM images with sample IDs top 3 highly impact insensitive left to right; (a) HMX CACs: 32 HMX/TATB, 8 HMX/HNS, & 58 HMX/PANi. (b) CL20 CACs: 57 CL20/ PANi, 34 CL-20/TATB, & S5 CL20/BCHMX. (c) BCHMX CACs: 33 BCHMX/TATB, 59 BCHMX/PANi, & 19 BCHMX/HNS. (d) RDX CACs: 35 RDX/TATB, 60 RDX/PANi, & 17 RDX/HNS (images regenerated from Refs. [15–22]). For sample codes compositions see Table 2.

The importance of the molar ratio of coformers in CACs is best documented on the CL20/BCHMX cocrystals (samples No. 32-38 in Table 1); the introduction of foreign molecules into the crystal lattice of CL20 tends to destabilize this nitramine (except perhaps for TATB and DATB), but in the case of the BCHMX coformer and for a molar ratio of 1.8/1.0, ECCs with surprisingly high resistance to impact can be obtained (sample No. 35 in Table 1, it in comparison with impact sensitivity of ε-CL20 and BCHMX).

### 3.8. Explosive properties

Researchers in the field of energetic cocrystals do not mention the well-known fact that the mixing of two explosives results in a mixture that usually has a higher detonation rate than would correspond to the percentage of components in this mixture [35]. The detonation energies were compared ($E_{deton}$) in the studies in this sense [15–21], which is summarized in Figs. 6-8.

Here, group "A" presents data of the brisant explosives (mostly CL20 and partly BCHMX) with the smallest effect of the increase in $E_{deton}$ values for the CACs, group "B" of co-agglomerates of RDX and HMX with coformers, having larger increases in these values, and the largest ever such effect is observed for group "C" with the PANi coformer.

All dependencies seem to intersect in a common intersection formed by the data of serial No's. 32-38 nitramine CACs from Table 4. For these nitraminic CACs alone, the effect of the mixture is opposite. Prof. Urbanski stated that these increases in values by the increase in entropy of the components entering the mixture [35]. For the nitraminic CACs, explained the decrease in the $E_{deton}$ values for their CACs by the decrease in entropy in the mixture of admittedly molecularly-structurally mutually different but chemically uniform coformers [17].

The well-known relationship between detonation velocities and charge densities of explosives is presented in Fig. 8. Here again, the set of CACs studied by us breaks down into group A of mostly pure nitramines

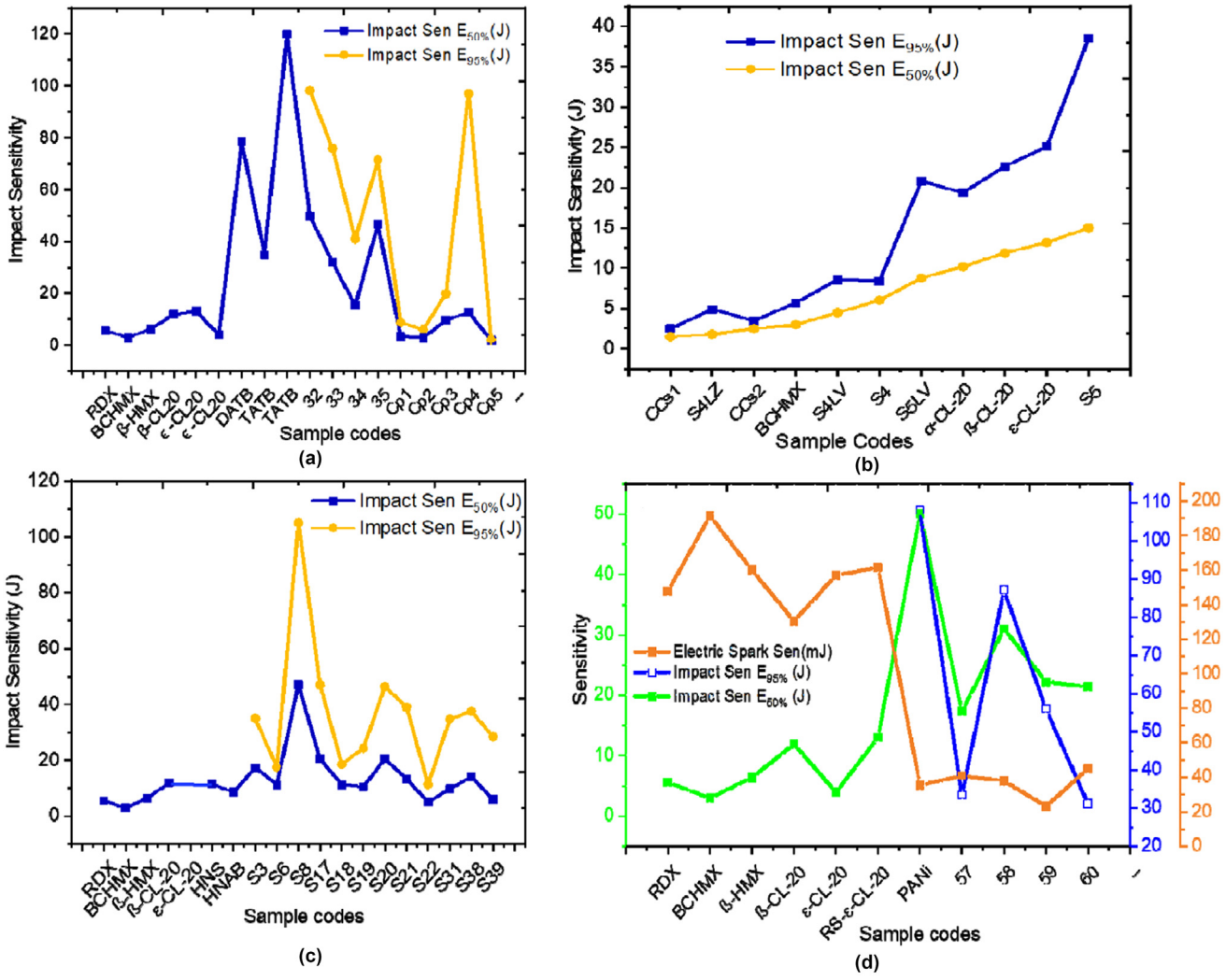


**Fig. 4.** A comparative graphical representation of impact and electrical spark sensitivities.

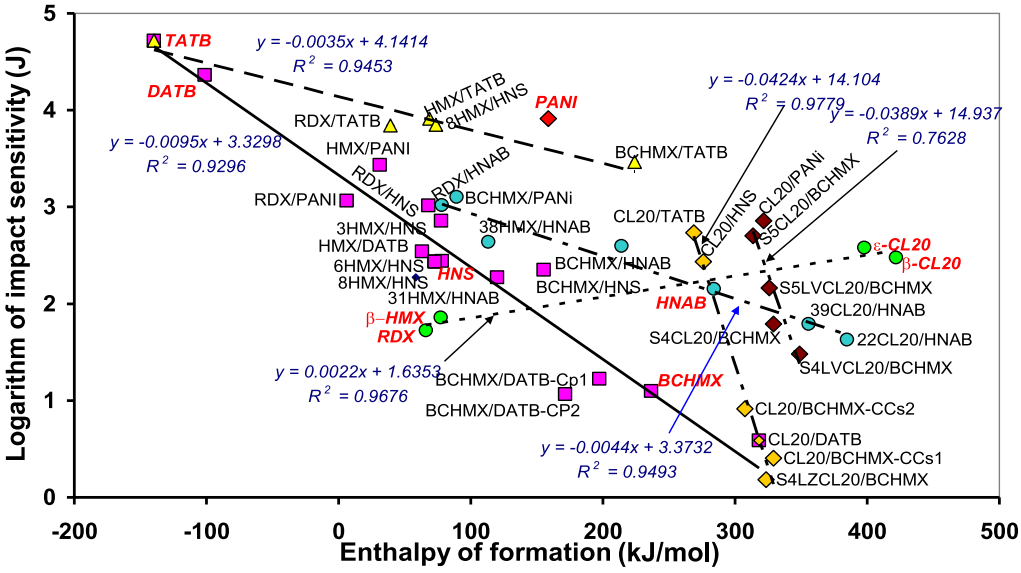


**Fig. 5.** The semi-logarithmic relationships between the impact sensitivity and energy content (represented by the enthalpy of formation) of the CACs prepared (data taken from papers [15–21]).

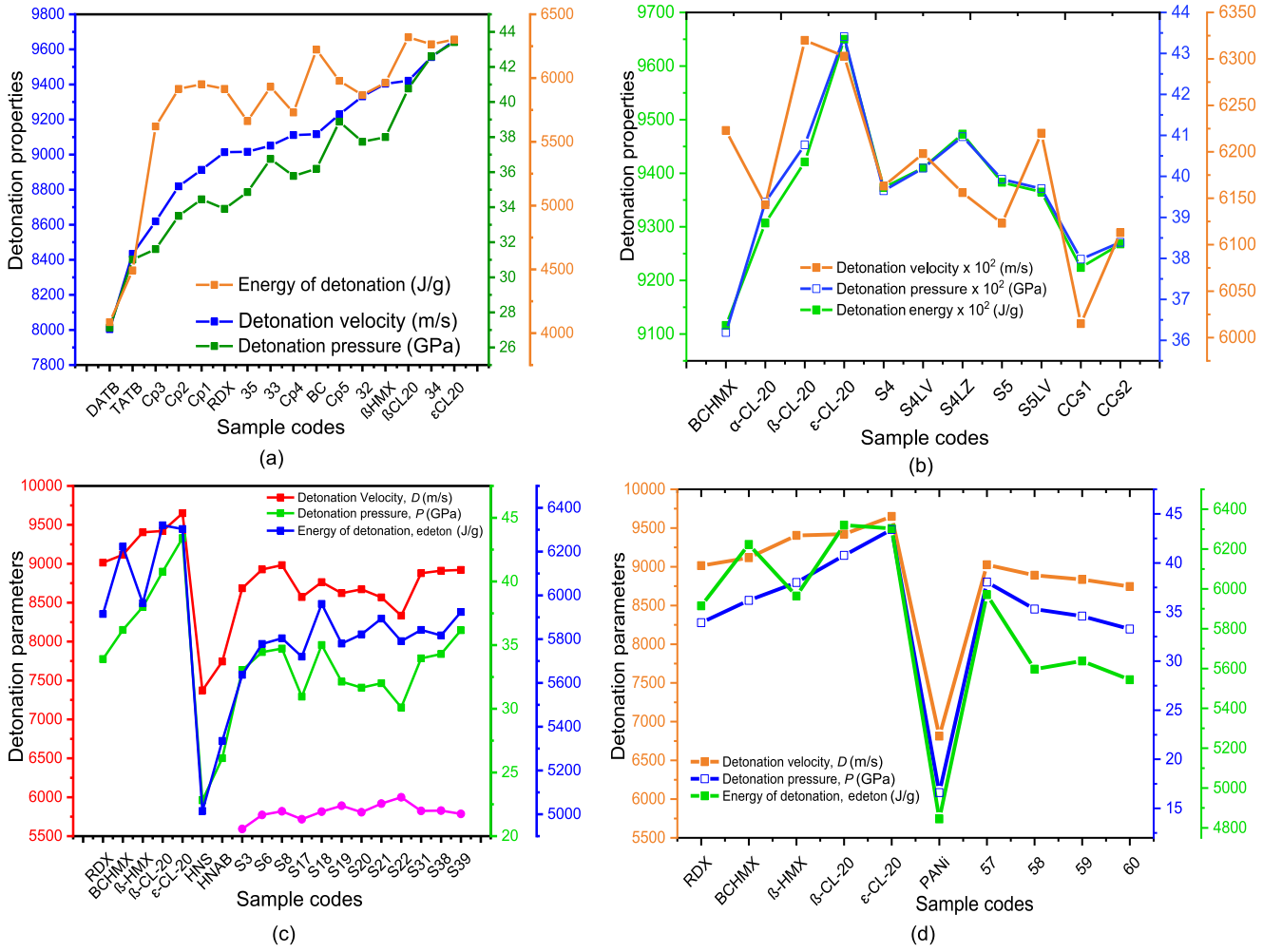


**Fig. 6.** Detonation parameters of CACs with pure nitramines used for preparation.

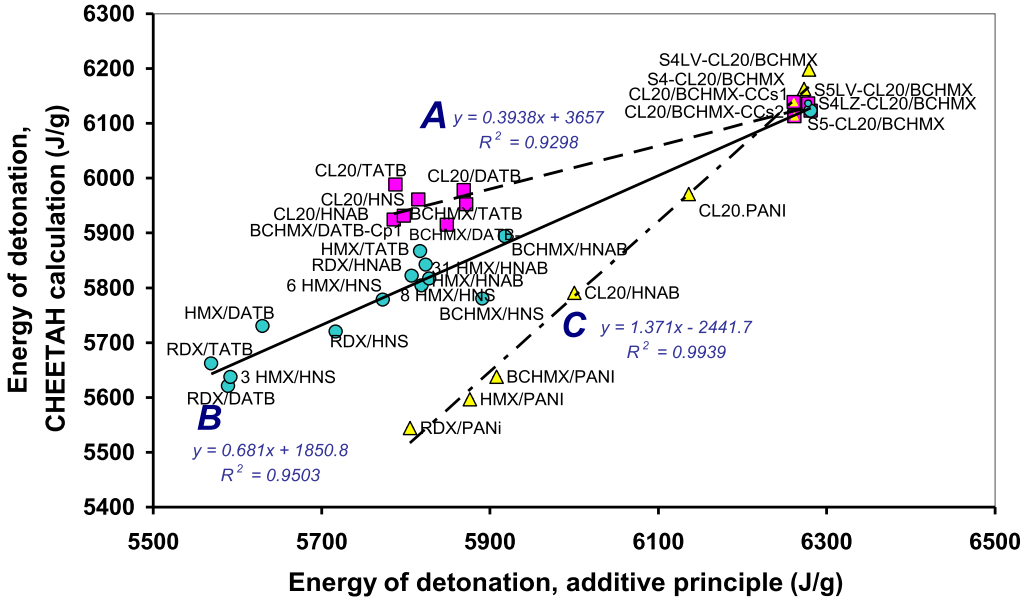


**Fig. 7.** The mutual relationships between the energies of detonation calculated on the basis of the additive principle (i.e., the percentage of components in the co-agglomerates) and that calculated by CHEETAH code [35] using experimental enthalpies of formation (data taken from papers [15–21]).

**Table 2**
Molecular formulas, thermochemical properties, and maximum crystal densities of pure substances and their corresponding CACs [15–22].

| Explosive | | | | | Heat of combustion | Enthalpy of formation | Crystal density | |
|---|---|---|---|---|---|---|---|---|
| No | Code design | Molar ratio NM/ CFs | Formula | Mol. weight | $Q_c$ (J/g) | $\Delta H_f$ (kJ/mol) | $\varrho$ (g/cm$^3$) | Refs. |
| 1 | RDX | – | $C_3H_6N_6O_6$ | 222.14 | 9522 | 66.2 | 1.810 | [14] |
| 2 | BCHMX | – | $C_4H_6N_8O_8$ | 294.17 | 9124 | 236.5 | 1.860 | [14] |
| 3 | $\beta$-HMX | – | $C_4H_8N_8O_8$ | 296.18 | 9485 | 77.3 | 1.902 | [14] |
| 4 | $\beta$-CL-20 | – | $C_6H_6N_{12}O_{12}$ | 438.23 | 8327 | 421.74 | 1.985 | [14] |
| 5 | ε-CL-20 | – | $C_6H_6N_{12}O_{12}$ | 438,23 | 8311 | 397.80 | 2.044 | [14] |
| 6 | TATB | – | $C_6H_6N_6O_6$ | 258.15 | 11,927 | −139.74 | 1.938 | [14] |
| 7 | DATB | – | $C_6H_5N_5O_6$ | 243.14 | 11,592 | −101.3 | 1.838 | [14] |
| 8 | HNS | – | $C_{14}H_6N_6O_{12}$ | 450.23 | 11,634 | 78.24 | 1.745 | [14] |
| 9 | HNAB | – | $C_{12}H_4N_8O_{12}$ | 452.21 | 12,384 | 284.09 | 1.799 | [14] |
| 10 | PANi | – | $([C_6H_4NH]_2[C_6H_4N]_2)_n$<br>$C_{6.00}H_{6.33}N_{0.98}O_{2.00}S_{0.14}$ | 95,800 [36]<br>128.64 | 24,497 | 158.57 | 1.5022 | [20] |
| 11 | 32 HMX/TATB | 1.00:0.12 | $C_{4.33}H_{8.00}N_{8.00}O_{8.00}$ | 300.09 | 9720 | 68.80 | 1.909 | [15] |
| 12 | 33 BCHMX/TATB | 1.00:0.37 | $C_{4.86}H_{4.86}N_{8.00}O_{8.00}$ | 303.33 | 9335 | 223.97 | 1.931 | [15] |
| 13 | 34 CL-20/TATB | 1.00:0.17 | $C_{7.01}H_{7.01}N_{12.00}O_{12.00}$ | 451.35 | 8927 | 268.76 | 2.033 | [15] |
| 14 | 35 RDX/TATB | 1.00:0.28 | $C_{3.65}H_{5.99}N_{6.00}O_{6.00}$ | 229.93 | 9660 | 39.12 | 1.869 | [15] |
| 15 | Cp1 BCHMX/DATB | 4.20:1.00 | $C_{4.72}H_{6.26}N_{8.00}O_{8.19}$ | 306.44 | 9627 | 197.37 | 1.851 | [14] |
| 16 | Cp2 BCHMX/DATB | 3.90:1.00 | $C_{4.76}H_{6.27}N_{8.000}O_{8.22}$ | 307.07 | 9579 | 171.46 | 1.831 | [14] |
| 17 | Cp3 RDX/DATB | 3.90:1.00 | $C_{3.66}H_{5.76}N_{6.00}O_{6.27}$ | 234.13 | 9919 | 58.33 | 1.793 | [14] |
| 18 | Cp4 $\delta$-HMX/DATB | 3.70:1.00 | $C_{4.79}H_{8.00}N_{8.00}O_{8.22}$ | 309.17 | 10,002 | 63.10 | 1.885 | [14] |
| 19 | Cp5 ß-CL-20/DATB | 2.20:1.00 | $C_{7.36}H_{7.81}N_{12.00}O_{13.74}$ | 484.20 | 9272 | 318.22 | 1.981 | [14] |
| 20 | 3 HMX/ HNS | 1.00:0.42 | $C_{7.54}H_{8.00}N_{8.00}O_{9.93}$ | 369.56 | 10,880 | 77.64 | 1.8730 | [18] |
| 21 | 6 HMX/ HNS | 1.00:0.16 | $C_{5.57}H_{8.00}N_{8.00}O_{8.85}$ | 328.60 | 10,386 | 72.78 | 1.8820 | [18] |
| 22 | 8 HMX/ HNS | 1.00:0.11 | $C_{5.09}H_{7.96}N_{8.00}O_{8.57}$ | 318.32 | 10,055 | 73.55 | 1.8778 | [18] |
| 23 | 17 RDX/ HNS | 1.00:0.14 | $C_{4.35}H_{6.00}N_{6.00}O_{6.73}$ | 250.02 | 10,040 | 68.10 | 1.7824 | [18] |
| 24 | 18 CL-20/ HNS | 1.00:0.61 | $C_{11.14}H_{7.40}N_{12.00}O_{14.80}$ | 546.15 | 10,444 | 275.89 | 1.9265 | [18] |
| 25 | 19 BCHMX/ HNS | 1.00:0.25 | $C_{5.89}H_{6.31}N_{8.00}O_{9.02}$ | 333.48 | 10,087 | 155.11 | 1.8278 | [18] |
| 26 | 20 RDX/ HNAB | 1.00:0.11 | $C_{3.90}H_{5.79}N_{6.00}O_{6.00}$ | 242.32 | 10,033 | 78.10 | 1.7831 | [18] |
| 27 | 21 BCHMX/ HNAB | 1.00:0.34 | $C_{6.44}H_{5.86}N_{8.00}O_{9.62}$ | 349.23 | 10,138 | 214.14 | 1.8267 | [18] |
| 28 | 22 CL-20/ HNAB | 1.00:0.46 | $C_{8.81}H_{6.00}N_{12.00}O_{13.40}$ | 494.35 | 9504 | 384.67 | 1.7918 | [18] |
| 29 | 31 HMX/ HNAB | 1.00:0.185 | $C_{5.25}H_{7.37}N_{8.00}O_{8.62}$ | 320.46 | 10,067 | 119.90 | 1.8467 | [18] |
| 30 | 38 HMX/ HNAB | 1.00:0.180 | $C_{5.22}H_{7.32}N_{8.00}O_{8.53}$ | 318.61 | 10,046 | 113.46 | 1.8575 | [18] |
| 31 | 39 CL-20/ HNAB | 1.00:0.37 | $C_{8.37}H_{6.00}N_{12.00}O_{13.18}$ | 485.54 | 9260 | 355.70 | 1.9411 | [18] |
| 32 | S4 CL20/BCHMX | 1.10:1.00 | $C_{6.00}H_{7.23}N_{12.00}O_{12.00}$ | 439.44 | 8475 | 329.00 | 1.9620 | [18] |
| 33 | S4LV CL20/BCHMX | 1.53:1.00 | $C_{6.00}H_{6.91}N_{12.00}O_{12.00}$ | 439.12 | 8446 | 348.87 | 1.9744 | [18] |
| 34 | S4LZ CL20/BCHMX | 1.52:1.00 | $C_{6.04}H_{6.89}N_{12.00}O_{12.00}$ | 439.58 | 8379 | 323.47 | 1.9745 | [18] |
| 35 | S5 CL20/BCHMX | 1.80:1.00 | $C_{6.00}H_{6.78}N_{12.00}O_{12.00}$ | 438.99 | 8343 | 313.62 | 1.9761 | [18] |
| 36 | S5LV CL20/BCHMX | 1.57:1.00 | $C_{5.99}H_{6.89}N_{12.00}O_{12.00}$ | 438.98 | 8318 | 325.89 | 1.9617 | [18] |
| 37 | CCs 1 CL20/BCHMX | 0.60:1.00 | $C_{6.03}H_{7.21}N_{12.00}O_{12.00}$ | 439.78 | 8447 | 329.13 | 1.9366 | [16] |
| 38 | CCs 2 CL20/BCHMX | 0.63:1.00 | $C_{6.00}H_{7.46}N_{12.00}O_{12.00}$ | 439.70 | 8655 | 307.45 | 1.9356 | [16] |
| 39 | 57 CL20/ PANi | [UP] | $C_{10..66}H_{11.01}N_{12.00}O_{14.62}S_{0.17}$ | 546.59 | 11,240 | 321.47 | 1.9691 | [20] |
| 40 | 58 HMX/PANi | [UP] | $C_{6.66}H_{10.16}N_{8.00}O_{9.02}S_{0.13}$ | 354.58 | 11,979 | 31.19 | 1.8967 | [20] |
| 41 | 59 BCHMX/PANi | [UP] | $C_{6.35}H_{8.00}N_{8.00}O_{8.82}S_{0.05}$ | 333.40 | 11,245 | 89.21 | 1.8916 | [20] |
| 42 | 60 RDX/PANi | [UP] | $C_{5.09}H_{8.60}N_{6.00}O_{6.71}S_{0.08}$ | 263.72 | 12,379 | 6.17 | 1.8295 | [20] |

**Note:** Here, UP- results under publication; materials.

(highly brisant explosives), into groups B and C of RDX, BCHMX and HMX co-agglomerates and into group C, formed by pure HNAB and HNS and also by CACs with CL20 content, in which coformers HNS, HNAB, PANi and DTAB significantly reduce the detonation rate. It is possible to see here, that HMX/TATB (data No. 11 in Table 4) with high resistance against impact should have detonation velocity near those of pure $\beta$-HMX. Another highly resistant against impact CAC, i. e. $\delta$-HMX/cis-HNS (data No. 22 in Table 4) is close to pure RDX in this sense.

### 3.9. Feasibility of co-agglomeration method

As shown by our results so far [15–21], the introduction of polynitro compound molecules into the crystal lattice of attractive nitramines usually leads to an increase in their initiation reactivity mainly for those with crowded molecules, but this can be partially eliminated by selection of the molar ratio in the resulting CAC. So far, the most effective "stabilizer" of these nitramines logically turns out to be TATB. Surprisingly, the coformer cis-HNS has a similar effect on the stabilization of $\delta$-HMX (here also the molar ratio of the coformers plays a major role), where, moreover, the microporosity of cis-HNS in the final CAC can turns out to be a significant positive factor. From an explosives' property point of view, the $\delta$-HMX/TATB co-agglomerate is the most advantageous, approaching pure $\beta$-HMX in its performance. Similarly, the best co-agglomerate $\delta$-HMX/cis-HNS, which is, however, in its performance closed logically to pure RDX.

Preparation of co-crystals by co-agglomeration (by "slurry method" co-crystallization) appears to be very interesting, giving products relatively high crystal density. It does not require initial coformers of defined granulometry - it is possible to apply components directly from their production after isolation from the reaction mixtures of their preparation and subsequent stabilization. Purification of coformers can take place in solution as part of their co-precipitation.

These preliminary results of ours also suggest that chemical engineering factors are involved in the preparation of CACs, as in con-

**Table 3**
Detonation properties of EECCs of attractive nitramines by traditional methods.

| Sr No | Energetic cocrystals (ECCs) | Detonation velocity, *D* (m/s) | Detonation pressure, *P* (p) | Refs. |
|---|---|---|---|---|
| 1 | CL20/BTF | 8969 | 39.10 | [37] |
| 2 | CL20/TNT | 8426 | 28.70 | [38] |
| 3 | CL20/DNB | 8434 | 34.07 | [39] |
| 4 | CL20/TNT | 8466 | 33.80 | [39] |
| 5 | CL20/MTNP | 9347 | 40.50 | [40] |
| 6 | CL20/AMTN | 8863 | NA | [25] |
| 7 | CL-20/2,4-MDNI | 8839 | 34.82 | [41] |
| 8 | CL-20/4,5-MDNI | 8919 | 35.69 | [41] |
| 9 | CL20/TNT | 8631 | NA | [42] |
| 10 | CL-20/DNDAP | 8997 | 37.50 | [43] |
| 11 | CL-20/TFAZ | 9103 | 37.20 | [44] |
| 12 | CL-20/ 2,4-DNI | 9324 | 39.20 | [45] |
| 13 | CL-20/1,4-DNI | 9242 | 39.01 | [46] |
| 14 | CL20/4,5-MDNI | 8604 | 34.45 | [47] |
| 15 | CL20/4,5-MDNI | 8972 | 38.59 | |
| 16 | HMX/ANPyO | 9444 | 41.03 | [46] |
| 17 | HMX/ANPyO | 9387 | 40.44 | [46] |
| 18 | HMX/BTNEN | 9380 | 42.95 | [48] |
| 19 | CL-20/TFAZ | 9103 | 37.20 | [44] |
| 20 | CL20/HMX | NA | NA | [49] |
| 21 | CL-20/HMX | NA | NA | [50] |
| 22 | CL-20/MTNI | 9093 | 37.46 | [51] |
| 23 | NBA:AmTz | 7280 | 19.50 | [52] |
| | NBA:TATOT | 7521 | 19.70 | |
| | NBA:NPTA | 6837 | 17.00 | |
| | NBA:DAG | 7685 | 20.90 | |
| 24 | 1:1 TT/HNT | 6091 | NA | [53] |
| 25 | 2:1 TT/HDNT | 5884 | NA | |
| 26 | 1:1 TT/TNP | 6903 | NA | |
| 27 | HNTO/AN | NA | NA | [54] |
| 28 | TNB/1,4-DNI | 7704 | 26.08 | [55] |
| 29 | TNB/DNMT | 7709 | 22.40 | |
| 30 | CL-20/HMX/MF | 9200 to 9250 | NA | [56] |
| 31 | CL-20/MTNP | 9347 | 40.50 | [57] |
| 32 | HMX/NTO composite | NA | NA | [58] |
| 33 | DNP/DAF | NA | NA | [59] |

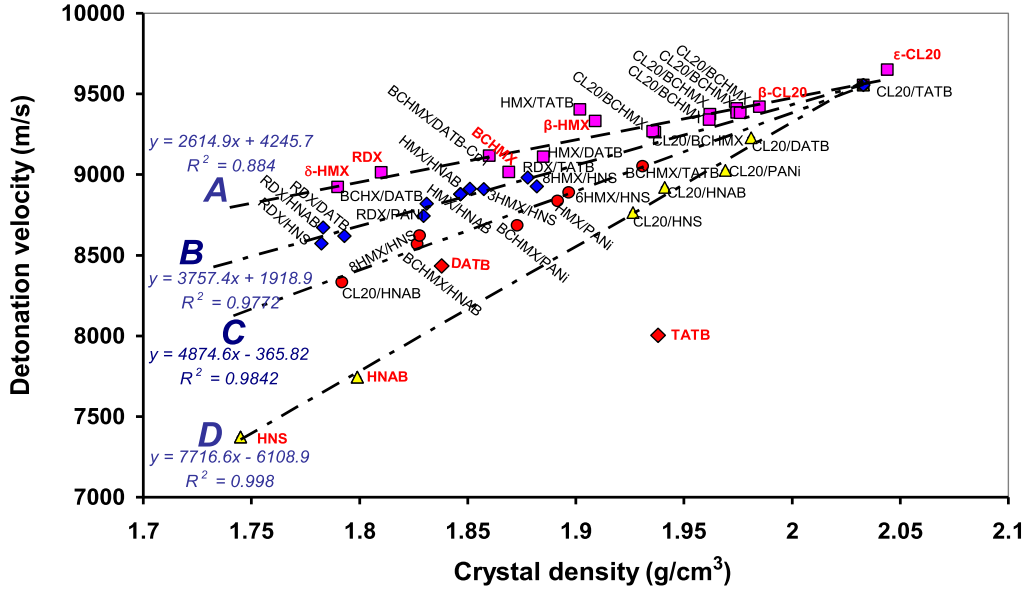


**Fig. 8.** The mutual relationships between the calculated detonation velocity for the maximal crystal density and this crystal density (data taken from papers [15–21]).

**Table 4**
Impact sensitivity and explosive properties of pure substances and corresponding CACs [15–22].

| Explosive | | Impact sensitivity $E_{dr}$ | | | | | | |
|---|---|---|---|---|---|---|---|---|
| Sr No | Code design | $E_{dr}$ 50% (J) | $E_{dr}$ 95 % (J) | Detonation velocity, $D$ (m/s) | Detonation pressure, $P$ (GPa) | Energy of detonation, $E_{deton}$ (J/g) | Additive value[a] of $E_{deton}$ (J/g) | Refs. |
| 1 | RDX | 5.6 | – | 9014 | 33.91 | 5915 | – | [14] |
| 2 | BCHMX | 3.0 | – | 9116 | 36.19 | 6223 | – | [14] |
| 3 | ß-HMX | 6.4 | – | 9404 | 38.00 | 5964 | – | [14] |
| 4 | ß-CL-20 | 11.9[b] | – | 9421 | 40.77 | 6320 | – | [14] |
| 5 | ε-CL-20 | 13.2[b]; 4.0 [c] | – | 9650 | 43.41 | 6303 | – | [14] |
| 6 | DATB | 78.5 | – | 8004 | 27.13 | 4086 | – | [14] |
| 7 | TATB | 112.0 | – | 8434 | 31.01 | 4492 | – | [14] |
| 8 | HNS (form I) | 11.5 | – | 7373 | 22.81 | 5015 | – | [14] |
| 9 | HNAB | 8.6 | – | 7744 | 26.12 | 5335 | – | [14] |
| 10 | PANi | 50.0 | 108.0 | 6813 | 16.61 | 6813 | 4845 | [20] |
| 11 | 32 δ-HMX/TATB | 50.0 | 98.3 | 9332 | 37.73 | 5867 | 5817 | [15] |
| 12 | 33 BCHMX/TATB | 32.0 | 76.0 | 9051 | 36.75 | 5931 | 5798 | [15] |
| 13 | 34 CL-20/TATB | 15.4 | 41.1 | 9556 | 42.60 | 6265 | 5788 | [15] |
| 14 | 35 RDX/TATB | 46.7 | 71.5 | 9016 | 34.86 | 5662 | 5569 | [15] |
| 15 | Cp1 BCHMX/DATB | 3.4 | 8.8 | 8913 | 34.45 | 5952 | 5872 | [14] |
| 16 | Cp2 BCHMX/DATB | 2.9 | 6.0 | 8819 | 33.50 | 5915 | 5849 | [14] |
| 17 | Cp3 RDX/DATB | 9.7 | 20.0 | 8619 | 31.61 | 5621 | 5589 | [14] |
| 18 | Cp4 δ-HMX/DATB | 12.7 | 97.2 | 9111 | 35.78 | 5730 | 5630 | [14] |
| 19 | Cp5 ß-CL-20/DATB | 1.8 | 2.1 | 9229 | 38.88 | 5978 | 5869 | [14] |
| 20 | 3 HMX/HNS | 17.4 | 35.0 | 8685 | 33.03 | 5637 | 5592 | [18] |
| 21 | 6 HMX/HNS | 11.4 | 17.6 | 8927 | 34.45 | 5778 | 5773 | [18] |
| 22 | 8 HMX/HNS | 47.0 | 105.1 | 8982 | 34.73 | 5804 | 5819 | [18] |
| 23 | 17 RDX/HNS | 20.4 | 47.0 | 8572 | 30.95 | 5720 | 5717 | [18] |
| 24 | 18 CL-20/HNS | 11.4 | 18.6 | 8764 | 35.01 | 5961 | 5815 | [18] |
| 25 | 19 BCHMX/HNS | 10.5 | 24.4 | 8622 | 32.13 | 5780 | 5891 | [18] |
| 26 | 20 RDX/HNAB | 20.5 | 46.4 | 8671 | 31.66 | 5822 | 5807 | [18] |
| 27 | 21 BCHMX/HNAB | 13.4 | 39.2 | 8568 | 32.01 | 5894 | 5918 | [18] |
| 28 | 22 CL-20/HNAB | 5.1 | 11.4 | 8333 | 30.11 | 5791 | 6000 | [18] |
| 29 | 31 HMX/HNAB | 9.7 | 34.8 | 8879 | 33.96 | 5842 | 5824 | [18] |
| 30 | 38 HMX/HNAB | 14.0 | 37.5 | 8911 | 34.30 | 5817 | 5828 | [18] |
| 31 | 39 CL-20/HNAB | 6.0 | 28.5 | 8921 | 36.17 | 5924 | 5786 | [18] |
| 32 | S4 CL20/BCHMX | 6.0 | 8.4 | 9373 | 39.65 | 6163 | 6273 | [16] |
| 33 | S4LV CL20/BCHMX | 4.4 | 8.6 | 9410 | 40.20 | 6198 | 6279 | [16] |
| 34 | S4LZ CL20/BCHMX | 1.2 | 4.9 | 9385 | 39.94 | 6136 | 6278 | [16] |
| 35 | S5 CL20/BCHMX | 14.9 | 38.5 | 9383 | 39.93 | 6123 | 6281 | [16] |
| 36 | S5LV CL20/BCHMX | 8.7 | 20.8 | 9341 | 39.41 | 6143 | 6279 | [16] |
| 37 | CCs1 CL20/BCHMX | 1.5 | – | 9262 | 38.43 | 6139 | 6261 | [16] |
| 38 | CCs2 CL20/BCHMX | 2.5 | – | 9268 | 38.39 | 6113 | 6262 | [16] |
| 39 | 57 CL20/ PANi | 17.4 | 33.4 | 9025 | 38,05 | 5971 | 5971 | [20] |
| 40 | 58 HMX/PANi | 31.0 | 87.2 | 8890 | 35,3 | 5597 | 5597 | [20] |
| 41 | 59 BCHMX/PANi | 22.3 | 55.9 | 8836 | 34,58 | 5638 | 5638 | [20] |
| 42 | 60 RDX/PANi | 21.4 | 31.1 | 8744 | 33,26 | 5544 | 5544 | [20] |

**Note:** (a) The value calculated on the basis of the additive principle, i.e., percentage of components in the co- agglomerate;
(b) The values for pure β-CL-20 and ε-CL-20, respectively, taken from paper [60];
(c) The value for "common" (technical) quality ε-CL-20.

ventional crystallization. With technical technological optimization this method is employable industrial scale cocrystal productions.

## 4. Concluding remarks

The developed a method that benefits nitramines cocrystal nano- and micro-particles. Key findings of interesting cocrystals are listed below.

(1) This method is practically a co-crystallization in suspension - "Slurry method", which considerably reduces the processing time and decreases the quantity of solvents compared to a solvent co-crystallization. It provides fine co-crystals of very good quality;
(2) Among the co-crystals of attractive cyclic nitramines with 1,3-diamino- and 1,3,5-triamino-2,4,6-trinitrobenzene, the ones with δ-HMX are very interesting, with a surprising result for coformer TATB with molar ratio 1.00/0.12 ($IS$ = 50 J, calculated $D$ = 9.3 km/s); however, TATB behaves here as an anticaking additive;
(3) Among the co-crystals of cyclic nitramines with cis-2,2′,4,4′,6,6′-hexanitrostilbene (HNS) and 2′,4,4′,6,6′-hexanitroazobenzene (HNAB), δ-HMX/cis-HNS with a molar ratio of 1.00/0.11 and $IS$ = 47 J (TNT has of 36.4 J) with calculated $D$ = 8.9 km/s stands out surprisingly; the impact resistance of this product far exceeds that one of both its coformers;
(4) The attempted co-agglomeration of sterically crowded nitramines ε-CL20 and BCHMX also resulted in a surprisingly good β-CL20/BCHMX product with a molar ratio of 1.8/1.0, $IS$ = 14.9 J and calculated $D$ = 9.4 km/s; also, here its impact resistance exceeds that one of both its coformers (mainly of BCHMX with $IS$ of 3 J);
(5) The molar ratio of the coformers and the choice of the continuous phase play a very important role in this co-agglomeration - the proteogenic one usually gives a better morphology than the aprotic medium; however, HNAB undergoes decomposition in the proteogenic solvent;
(6) In all co-crystal types studied, HMX was specified in its δ-modification, CL20 in its β-modification and HNS in its cis-conformation; it is the spatially similar orientation of the δ-HMX and cis-HNS molecules that could be one of the reasons for the surprisingly low sensitivity of the δ-HMX/cis-HNS co-crystal for the molar ratio of coformers 1.00/0.11;

(7) The polyaniline (PANi) given a unique combination of CACs in which they are impact insensitive (+5 J to 25 J) and electric spark (-100 mJ to 150 mJ) and laser (29 mV with 10×/0.25 grating) sensitive, with relatively better physiochemical properties and detonation properties. Especially HMX (impact sensitivity 31 J from original of 6.4 J), which is present in the composite in its $\alpha$-modification, which is in its pure state extremely sensitive to impact (1.9 J);

(8) The very well-known phenomenon of higher detonation parameters of explosives mixtures compared to their parameters, calculated on the basis of the percentage of components in the mixture, is valid for co-crystals with DATB and TATB, for co-crystals containing cis-HNS and HNAB there is not such a significant difference, and the opposite finding was found for cocrystals $\beta$-CL20/BCHMX.

## Declaration of interests

There are no conflicts to declare.

## Declaration of competing interest

The authors declare that they have no known competing financial interests or personal relationships that could have appeared to influence the work reported in this paper.

## Acknowledgments

Author V. B. Patil is gratefully thankful to research funding from the Students Grant of the Faculty of Chemical Technology at the University of Pardubice.

## References

[1] O.T. O'Sullivan, M.J. Zdilla, Properties and promise of catenated nitrogen systems as high-energy-density materials, Chem. Rev. 120 (2020) 5682–5744, doi:10.1021/acs.chemrev.9b00804.
[2] P.F. Pagoria, G.S. Lee, A.R. Mitchell, R.D. Schmidt, A review of energetic materials synthesis, Thermochim. Acta 384 (2002) 187–204, doi:10.1016/S0040-6031(01)00805-X.
[3] J. Sabatini, K. Oyler, Recent advances in the synthesis of high explosive materials, Crystals 6 (2015) 5 (Basel), doi:10.3390/cryst6010005.
[4] J. Chen, J. Tang, H. Xiong, H. Yang, G. Cheng, Combining triazole and furazan frameworks via methylene bridges for new insensitive energetic materials, Energ. Mater. Front. 1 (2020) 34–39, doi:10.1016/j.enmf.2020.07.001.
[5] Y. Zheng, X. Zhao, X. Qi, K. Wang, T. Liu, Synthesis of 5-(1H-pyrazol-1-yl)-2H-tetrazole-derived energetic salts with high thermal stability and low sensitivity, Energ. Mater. Front. 1 (2020) 83–89, doi:10.1016/j.enmf.2020.08.004.
[6] R. Bu, F. Jiao, G. Liu, J. Zhao, C. Zhang, Categorizing and understanding energetic crystals, Cryst. Growth Des. 21 (2021) 3–15, doi:10.1021/acs.cgd.0c01300.
[7] U. Teipel, J.K. Bremser, Particle characterization, in: Energetic Materials, John Wiley & Sons, Ltd,, 2004, pp. 293–332, doi:10.1002/3527603921.ch8.
[8] C. Zhang, F. Jiao, H. Li, Crystal engineering for creating low sensitivity and highly energetic materials, Cryst. Growth Des. 18 (2018) 5713–5726, doi:10.1021/acs.cgd.8b00929.
[9] F. Jiao, Y. Xiong, H. Li, C. Zhang, Alleviating the energy & safety contradiction to construct new low sensitivity and highly energetic materials through crystal engineering, CrystEngComm 20 (2018) 1757–1768, doi:10.1039/C7CE01993A.
[10] X.X. Zhang, Z.J. Yang, F. Nie, Q.L. Yan, Recent advances on the crystallization engineering of energetic materials, Energ. Mater. Front. 1 (2020) 141–156, doi:10.1016/j.enmf.2020.12.004.
[11] C. Zhang, Y. Cao, H. Li, Y. Zhou, J. Zhou, T. Gao, H. Zhang, Z. Yang, G. Jiang, Toward low-sensitive and high-energetic cocrystal I: evaluation of the power and the safety of observed energetic cocrystals, CrystEngComm 15 (2013) 4003–4014, doi:10.1039/c3ce40112j.
[12] M. Sultan, J. Wu, I.U. Haq, M. Imran, L. Yang, J. Wu, J. Lu, L. Chen, Recent progress on synthesis, characterization, and performance of energetic cocrystals: a review, Molecules 27 (2022) 4775, doi:10.3390/molecules27154775.
[13] H.R. Pouretedal, S. Damiri, A. Zandi, Study the operating conditions on agglomeration of RDX particles in anti-solvent crystallization by using statistical optimization, Def. Technol. 15 (2019) 233–240, doi:10.1016/j.dt.2018.09.007.
[14] X. Zhao, M. Zhang, W. Qian, F. Gong, J. Liu, Q. Zhang, Z. Yang, Interfacial engineering endowing energetic co-particles with high density and reduced sensitivity, Chem. Eng. J. 387 (2020) 124209, doi:10.1016/j.cej.2020.124209.
[15] V.B. Patil, K. Zalewski, J. Schuster, P. Belina, W. Trzcinski, S. Zeman, A new insight into the energetic co-agglomerate structures of attractive nitramines, Chem. Eng. J. 420 (2021), doi:10.1016/j.cej.2021.130472.
[16] V.B. Patil, P. Bělina, W.A. Trzcinski, S. Zeman, Preparation and properties of co-mixed crystals of 1,3-di- and 1,3,5-tri-amino-2,4,6-trinitrobenzenes with attractive cyclic nitramines, J. Ind. Eng. Chem. 115 (2022) 135–146, doi:10.1016/j.jiec.2022.07.043.
[17] V.B. Patil, Q.L. Yan, W.A. Trzciński, P. Bělina, J. Shánělová, T. Musil, S. Zeman, Co-agglomerated crystals of cyclic nitramines with sterically crowded molecules, CrystEngComm (2022) 10.1039.D2CE00840H, doi:10.1039/D2CE00840H.
[18] V.B. Patil, R. Svoboda, S. Zeman, Thermal studies on performance of DATB and TATB coagglomerated crystals, Thermochim. Acta 724 (2023) 179494, doi:10.1016/j.tca.2023.179494.
[19] V.B. Patil, P. Bělina, W.A. Trzcinski, S. Zeman, Co-agglomerated crystals of 2,2′,4,4′,6,6′-hexanitro -stilbene/-azobenzene with attractive nitramines, Chem. Eng. J. 457 (2023) 141200, doi:10.1016/j.cej.2022.141200.
[20] V.B. Patil, O. Machalický, P. Bělina, R. Svoboda, W.A. Trzcinski, S. Zeman, Co-agglomerated - polyaniline composite crystals of attractive nitramines -manuscript under communication, (March 2024).
[21] M. Novák, Ověření Vlivu bicyklo-HMX Na Parametry Prachu s Obsahem RDX (Verification of the bicyclo-HMX Effect On the RDX Gunpowder parameters), The Final Project of the Licensing Study, University of Pardubice, 2022.
[22] V.B. Patil, R. Svoboda, P. Belina, Thermal studies of attractive nitramines/polyaniline composite crystals prepared via co-agglomeration, in: New Trends in Research of Energetic Materials (NTREM, 2023, University of Pardubice, Czech Republic, 2023, pp. 419–431.
[23] B. Tian, Y. Xiong, L. Chen, C. Zhang, Relationship between the crystal packing and impact sensitivity of energetic materials, CrystEngComm 20 (2018) 837–848, doi:10.1039/C7CE01914A.
[24] G. Liu, S. Wei, C. Zhang, Review of the intermolecular interactions in energetic molecular cocrystals, Cryst. Growth Des. 20 (2020) 7065–7079, doi:10.1021/acs.cgd.0c01097.
[25] X. Zhang, S. Chen, Y. Wu, S. Jin, X. Wang, Y. Wang, F. Shang, K. Chen, J. Du, Q. Shu, A novel cocrystal composed of CL-20 and energetic ionic salt, Chem. Commun. 54 (2018) 13268–13270, doi:10.1039/C8CC06540C.
[26] R. Bu, Y. Xiong, C. Zhang, pi-pi stacking contributing to the low or reduced impact sensitivity of energetic materials, Cryst. Growth Des. 20 (2020) 2824–2841, doi:10.1021/acs.cgd.0c00367.
[27] S. Li, R. Gou, C. Zhang, n−$\pi$ Stacking in Energetic Crystals, Cryst Growth Des 22 (2022) 1991–2000, doi:10.1021/acs.cgd.2c00034.
[28] V.B. Patil, M.N. Nadagouda, S.A. Ture, C. Yelamaggad, A. Venkataraman, Detection of energetic materials via polyaniline and its different modified forms, Polym. Adv. Technol. 32 (2021) 4663–4677, doi:10.1002/pat.5458.
[29] V.B. Patil, S.A. Ture, C.V. Yelamaggad, M.N. Nadagouda, A. Venkataraman, Turn-off fluorescent sensing of energetic materials using protonic acid doped polyaniline: a spectrochemical mechanistic approach, Z .Anorg. Allg. Chem. 647 (2021) 331–340, doi:10.1002/zaac.202000321.
[30] R.E. Cobbledick, R.W.H. Small, The crystal structure of the $\delta$-form of 1,3,5,7-tetranitro-1,3,5,7-tetraazacyclooctane ($\delta$-HMX), Acta Crystallogr. B 30 (1974) 1918–1922, doi:10.1107/S056774087400611X.
[31] H. Zhang, Y. Liu, S. Li, S. Huang, J. Xu, H. Zhang, J. Li, S. Yang, Three-dimensional hierarchical 2,2,4,4,6,6-hexanitrostilbene crystalline clusters prepared by controllable supramolecular assembly and deaggregation process, CrystEngComm 18 (2016) 7940–7944, doi:10.1039/C6CE01292B.
[32] H.H. Licht, Performance and sensitivity of explosives, Propellants Explos. Pyrotech. 25 (2000) 126–132, doi:10.1002/1521-4087(200006)25:3<126::AID-PREP126>3.0.CO;2-8.
[33] S. Zeman, The influence of energy content and its outputs on the impact sensitivity of high-nitrogen energetic materials, J. Energ. Mater. 40 (2022) 1–14 Journal of Energetic Materials, doi:10.1080/07370652.2020.1822463.
[34] S. Zeman, M. Jungová, Sensitivity and performance of energetic materials, Propellants Explos. Pyrotech. 41 (2016) 426–451, doi:10.1002/prep.201500351.
[35] L.E. Fried, CHEETAH 1.39 Users' Manual UCRL-MA-117541, Lawrence Livermore National Laboratory, CA, 1996.
[36] H.S. Kolla, S.P. Surwade, X. Zhang, A.G. MacDiarmid, S.K. Manohar, Absolute molecular weight of polyaniline, J. Am. Chem. Soc. 127 (2005) 16770–16771, doi:10.1021/ja055327k.
[37] Z. Yang, H. Li, X. Zhou, C. Zhang, H. Huang, J. Li, F. Nie, Characterization and properties of a novel energetic–energetic cocrystal explosive composed of HNIW and BTF, Cryst. Growth Des. 12 (2012) 5155–5158, doi:10.1021/cg300955q.
[38] Z. Yang, H. Li, H. Huang, X. Zhou, J. Li, F. Nie, Preparation and performance of a HNIW/TNT cocrystal explosive, Propellants Explos. Pyrotech. 38 (2013) 495–501, doi:10.1002/prep.201200093.
[39] Y. Wang, Z. Yang, H. Li, X. Zhou, Q. Zhang, J. Wang, Y. Liu, A novel cocrystal explosive of HNIW with good comprehensive properties, Propellants Explos. Pyrotech. 39 (2014) 590–596, doi:10.1002/prep.201300146.
[40] Q. Ma, T. Jiang, Y. Chi, Y. Chen, J. Wang, J. Huang, F. Nie, A novel multi-nitrogen 2,4,6,8,10,12-hexanitrohexaazaisowurtzitane-based energetic co-crystal with 1-methyl-3,4,5-trinitropyrazole as a donor: experimental and theoretical investigations of intermolecular interactions, New J. Chem. 41 (2017) 4165–4172, doi:10.1039/c6nj03976f.

[41] Z. Yang, H. Wang, Y. Ma, Q. Huang, J. Zhang, F. Nie, J. Zhang, H. Li, Isomeric cocrystals of CL-20: a promising strategy for development of high-performance explosives, Cryst. Growth Des. 18 (2018) 6399–6403, doi:10.1021/acs.cgd.8b01068.
[42] Y. Liu, C. An, J. Luo, J. Wang, High-density HNIW/TNT cocrystal synthesized using a green chemical method, Acta Crystallogr. Sect. B Struct. Sci. Cryst. Eng. Mater. 74 (2018) 385–393, doi:10.1107/S2052520618008442.
[43] N. Liu, B. Duan, X. Lu, H. Mo, M. Xu, Q. Zhang, B. Wang, Preparation of CL-20/DNDAP cocrystals by a rapid and continuous spray drying method: an alternative to cocrystal formation, CrystEngComm 20 (2018) 2060–2067, doi:10.1039/c8ce00006a.
[44] N. Liu, B.H. Duan, X.M. Lu, B.Z. Wang, Investigation of CL-20/TFAZ cocrystal: preparation, structure and performance, J. Phys. Conf. Ser. 1721 (2021) 012005, doi:10.1088/1742-6596/1721/1/012005.
[45] J. Liu, Z. Yan, D. Chi, L. Yang, Synthesis of the microspheric cocrystal CL-20/2,4-DNI with high energy and low sensitivity by a spray-drying process, New J. Chem. 43 (2019) 17390–17394, doi:10.1039/C9NJ04731J.
[46] Y. Tan, Z. Yang, H. Wang, H. Li, F. Nie, Y. Liu, Y. Yu, High energy explosive with low sensitivity: a new energetic cocrystal based on CL-20 and 1,4-DNI, Cryst. Growth Des. 19 (2019) 4476–4482, doi:10.1021/acs.cgd.9b00250.
[47] Y. Tan, Y. Liu, H. Wang, H. Li, F. Nie, Z. Yang, Different stoichiometric ratios realized in energetic–energetic cocrystals based on CL-20 and 4,5-MDNI: a smart strategy to tune performance, Cryst. Growth Des. 20 (2020) 3826–3833, doi:10.1021/acs.cgd.0c00138.
[48] N. Zohari, F. Mohammadkhani, M. Montazeri, S. Roosta, S. Hosseini, M. Zaree, Synthesis and characterization of a novel explosive HMX/BTNEN (2:1) cocrystal, Propellants Explos. Pyrotech. 46 (2021) 329–333, doi:10.1002/prep.202000202.
[49] D. Herrmannsdörfer, T.M. Klapötke, Semibatch reaction crystallization for scaled-up production of high-quality CL-20/HMX cocrystal: efficient because of solid dosing, Cryst. Growth Des. 21 (2021) 1708–1717, doi:10.1021/acs.cgd.0c01611.
[50] L. Li, H. Ling, J. Tao, C. Pei, X. Duan, Microchannel-confined crystallization: shape-controlled continuous preparation of a high-quality CL-20/HMX cocrystal, CrystEngComm 24 (2022) 1523–1528, doi:10.1039/D1CE01524A.
[51] P. Lian, L. Zhang, H. Su, J. Chen, L. Chen, J. Wang, A novel energetic cocrystal composed of CL-20 and 1-methyl-2,4,5-trinitroimidazole with high energy and low sensitivity, Acta Crystallogr. B Struct. Sci. Cryst. Eng. Mater. 78 (2022) 133–139, doi:10.1107/S2052520622000245.
[52] A.K. Yadav, V.D. Ghule, S. Dharavath, Thermally stable and insensitive energetic cocrystals comprising nitrobarbituric acid coformers, Cryst. Growth Des. 23 (2023) 2826–2836, doi:10.1021/acs.cgd.3c00016.
[53] P. Peng, N. Ding, C. Zhao, Y. Li, J. Liu, S. Li, S. Pang, Improving the stability of all-carbon-nitrated azoles through cocrystallization, Cryst. Growth Des. 22 (2022) 2158–2167, doi:10.1021/acs.cgd.1c01237.
[54] A. Abdelaziz, A. Tarchoun, H. Boukeciat, D. Trache, Insight into the thermodynamic properties of promising energetic HNTO·AN Co-crystal: heat capacity, combustion energy, and formation enthalpy, Energies 15 (2022) 6722 (Basel), doi:10.3390/en15186722.
[55] S. Qiao, J. Wang, Y. Yu, Y. Liu, Z. Yang, H. Li, Two novel TNB energetic cocrystals with low melting point: a potential strategy to construct melt cast explosive carriers, CrystEngComm 24 (2022) 2948–2953, doi:10.1039/D2CE00025C.
[56] B. Duan, X. Lu, H. Mo, B. Tan, B. Wang, N. Liu, Fabrication of CL-20/HMX Cocrystal@Melamine–formaldehyde resin core–shell composites featuring enhanced thermal and safety performance via *in situ* polymerization, IJMS 23 (2022) 6710, doi:10.3390/ijms23126710.
[57] F. Yang, Z. Yang, Q. Yu, G. Li, C. Zhao, Y. Tian, Thermal escape" of MTNP: the phase separation of CL-20/MTNP cocrystals under long-term heating, Phys. Chem. Chem. Phys. 25 (2023) 6838–6846, doi:10.1039/D2CP04822A.
[58] H. Zhao, G. Gu, J. Shen, X. Zhao, J. Wang, G. Lan, Preparation of spherical HMX/DMF solvates, spherical HMX particles, and HMX@NTO composites: a way to reduce the sensitivity of HMX, ACS Omega 8 (2023) 14041–14046, doi:10.1021/acsomega.3c00606.
[59] Q.N. Tariq, Y. Bi, S. Manzoor, M.N. Tariq, W.L. Cao, W.S. Dong, J.G. Zhang, Synthesis, performance, and thermal behavior of two insensitive 3,4-dinitropyrazole-based energetic cocrystals, Cryst. Growth Des. 23 (2023) 112–119, doi:10.1021/acs.cgd.2c00809.
[60] Y. Ou, C. Wang, Z. Pan Z, B. Chen, Sensitivity of hexanitrohexaazaisowurtzitane, J. Energy Mater 7 (1999) 100–108 )..